

Analysis of the precipitation process of secondary phases after long-term ageing of S304H steel

Adam ZIELIŃSKI¹, Robert WERSTA², and Marek SROKA^{3*}

¹Łukasiewicz Research Network – Institute for Ferrous Metallurgy, ul. K. Miarki 12-14, 44-100 Gliwice, Poland

²Office of Technical Inspection, Regional Branch Office based in Wrocław, ul. Grabiszyńska 51, 53-503 Wrocław, Poland

³Department of Engineering Materials and Biomaterials, Silesian University of Technology, ul. Konarskiego 18a, 44 100 Gliwice, Poland

Abstract. S304H steel is used in the construction of pressure components of boilers with supercritical operating parameters. The paper presents the results of research on the microstructure following ageing for 30 000 hours at 650 and 700°C. Microstructure examination was performed using scanning and transmission electron microscopy. The precipitates were identified using transmission electron microscopy. The paper analyses the precipitation process and its dynamics depending on the temperature and ageing time in detail. MX carbonitrides and the ϵ -Cu phase were proved to be the most stable phase, regardless of the test temperature. It was also showed that the $M_{23}C_6$ carbide precipitates in the tested steel and the intermetallic sigma phase (σ) may play a significant role in the loss of durability of the tested steel. This is related to their significant increase due to the influence of elevated temperature, and their coagulation and coalescence dynamics strongly depend on the ageing/operating temperature level. The qualitative and quantitative identification of the secondary phase precipitation processes described in the study is important in the analysis of the loss of durability of the tested steel under creep conditions.

Key words: S304H steel; microstructure; precipitates; ageing; loss of durability.

1. INTRODUCTION

The continuous increase of energy demand in Poland requires not only further development of conventional energy sources, but also maintenance of the current state. Poland's energy policy assumes that by 2040 over 50% of electricity in the country will come from fossil fuels (hard and brown coal) [1, 2]. Therefore, it is important to know the effect of long-term influence of elevated and high temperature on the stability of functional properties of pressure equipment of power units [3–11]. Materials used for devices operating in the power, chemical, petrochemical or aviation industries should be characterized by increased properties under the conditions of long-term exposure to high temperature, stress and aggressive environment [12–14]. This applies particularly to components operating under supercritical temperature and stress conditions, i.e. creep and fatigue conditions. The knowledge of the precipitation processes has a significant impact not only on the modification of the chemical composition when designing new steels and alloys for operation at elevated and high temperatures. It also provides significant information on the safe operation of multi-million investments in the conventional power industry [15–18].

2. MATERIAL AND METHODOLOGY

The fine-grained S304H steel, which is the subject of the research, was developed as a result of modification of classic austenitic 304 steel (X8CrNi18-8). This material is an austenitic chromium-nickel steel with the addition of copper, with an average chromium content of approx. 18%, nickel at 9% and copper at 2%, resistant to corrosion. The steel shows high creep strength as compared to other high-alloy steels, which is 68 MPa at 700°C for 100 000 h. High creep resistance results from the strong solution and precipitation hardening. The creep strength value is a good recommendation for the use of steel in boilers with supercritical steam parameters. In the power industry, steel is intended for seamless pipes for applications in the temperature range of up to 700°C. When used for pressure equipment, pipes should meet the requirements of Directive 2014/68/EU, Chapter 4, Annex I. The chemical composition of the tested S304H steel (Table 1) as well as the melt and control analysis of the product provided by the manufacturer in the tubes certificate should be consistent with the requirements contained in Table 2.

In order to carry out qualitative and quantitative analysis of secondary phase precipitates in S304H steel, metallographic tests of such steel were performed after ageing at 650 and 700°C for 1000, 10 000 and 30 000 h.

The microstructure studies were carried out using an Inspect F scanning electron microscope (SEM) on electrolytically etched microsection and transmission electron microscopy (S/TEM) with the use of thin films. Changes in the microstructure

*e-mail: marek.sroka@polsl.pl

Manuscript submitted 2021-03-01, revised 2021-04-15, initially accepted for publication 2021-05-07, published in October 2021

Table 1
Chemical composition of the material of the tested S304H steel tube

	Chemical composition, [wt %]											
	C	Si	Mn	P	S	Cu	Cr	Ni	Nb	B	N	Al
Follow-up	0.09	0.20	0.80	0.003	0.001	2.99	18.4	8.80	0.48	0.004	0.11	0.006

Table 2
Melt analysis of S304H steel as per PN-EN 10216-5 2013

		Chemical composition, [wt %]											
		C	Si	Mn	P	S	Cr	Ni	Nb	Cu	N	Al	B
Melt analysis	min	0.07	–	–	–	–	17.0	7.5	0.30	2.50	0.05	0.003	0.001
	max	0.13	0.30	1.0	0.04	0.01	19.0	10.5	0.60	3.50	0.12	0.030	0.01
Product analysis	min	–	–	–	–	–	16.80	7.4	0.25	2.45	0.4	0.003	0.0007
	max	0.14	0.35	1.04	0.045	0.018	19.20	10.6	0.65	3.55	0.13	0.030	0.0103

during long-term ageing, mainly related to the precipitation processes of secondary phases, were analyzed. Qualitative analysis and statistical quantitative evaluation of precipitates of the main secondary ϵ -Cu and $M_{23}C_6$ phases and the σ phase were performed.

The study of the substructure and identification of the precipitates were carried out with the use of an FEI Titan 80–300 high-resolution transmission electron microscope using thin films. This microscope is equipped with a STEM scanning system and BF, DF and HAADF scanning-transmission detectors, a Cs condenser spherical aberration corrector, and an EDS energy dispersion spectrometer. Preparations for TEM tests were prepared in a FIB tool.

Quantitative analysis of the precipitates was carried out with the use of a computer image analysis system, based on the images of microstructure captured using a scanning and transmission electron microscope. The image analysis system was calibrated using a scale marker placed on microstructure images. A fixed measuring frame with the dimensions of 1020×940 pixels was used.

3. TEST RESULTS AND ANALYSIS

As delivered, the tested steel is characterized by a fine-grained austenitic structure with grain size of 7–9 according to ASTM standards (Fig. 1) and visible annealing twins with coherent and non-coherent boundaries and single primary NbCN (MX) precipitates of various sizes, distributed inside the grains.

The fine-grained structure provides the steel with good ductility, expressed in impact strength, as well as strength and plasticity. Moreover, it positively influences the resistance to oxidation in comparison to coarse grain steels [19, 20]. Detailed studies of the microstructure of S304H steel after long-term ageing were focused on the observation of precipitation processes related to the initial stages of precipitation ($M_{23}C_6$, σ phase), precipitation along grain boundaries and changes in the morphology of secondary phases.

Representative images of the microstructure after long-term ageing, observed on a scanning microscope, are shown in Fig. 2.

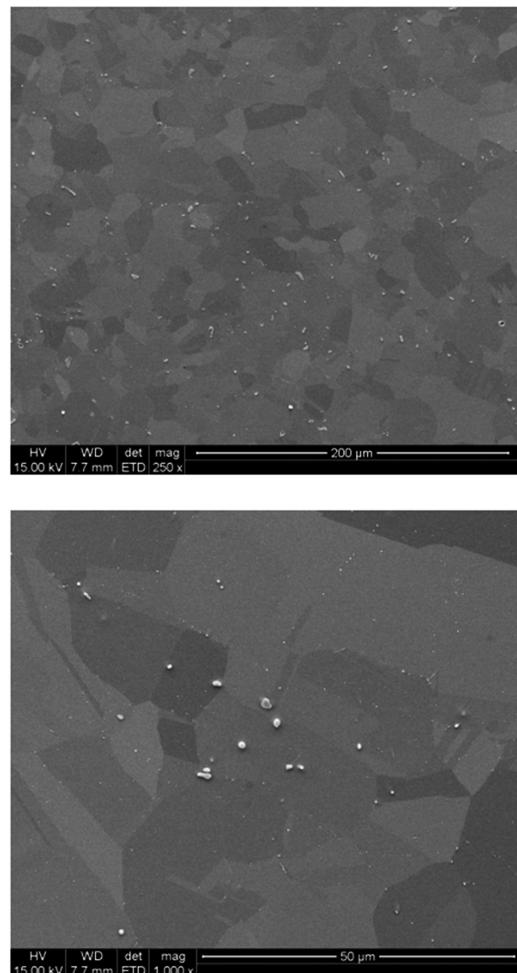


Fig. 1. Microstructure of as-delivered S304H steel, SEM

In order to analyze the precipitation processes of the finely-dispersed ϵ -Cu phase, the substructure was observed at high magnifications in a transmission electron microscope. An example of the identified ϵ -Cu phase and its morphology after ageing, used for statistical analysis, is shown in Fig. 3.

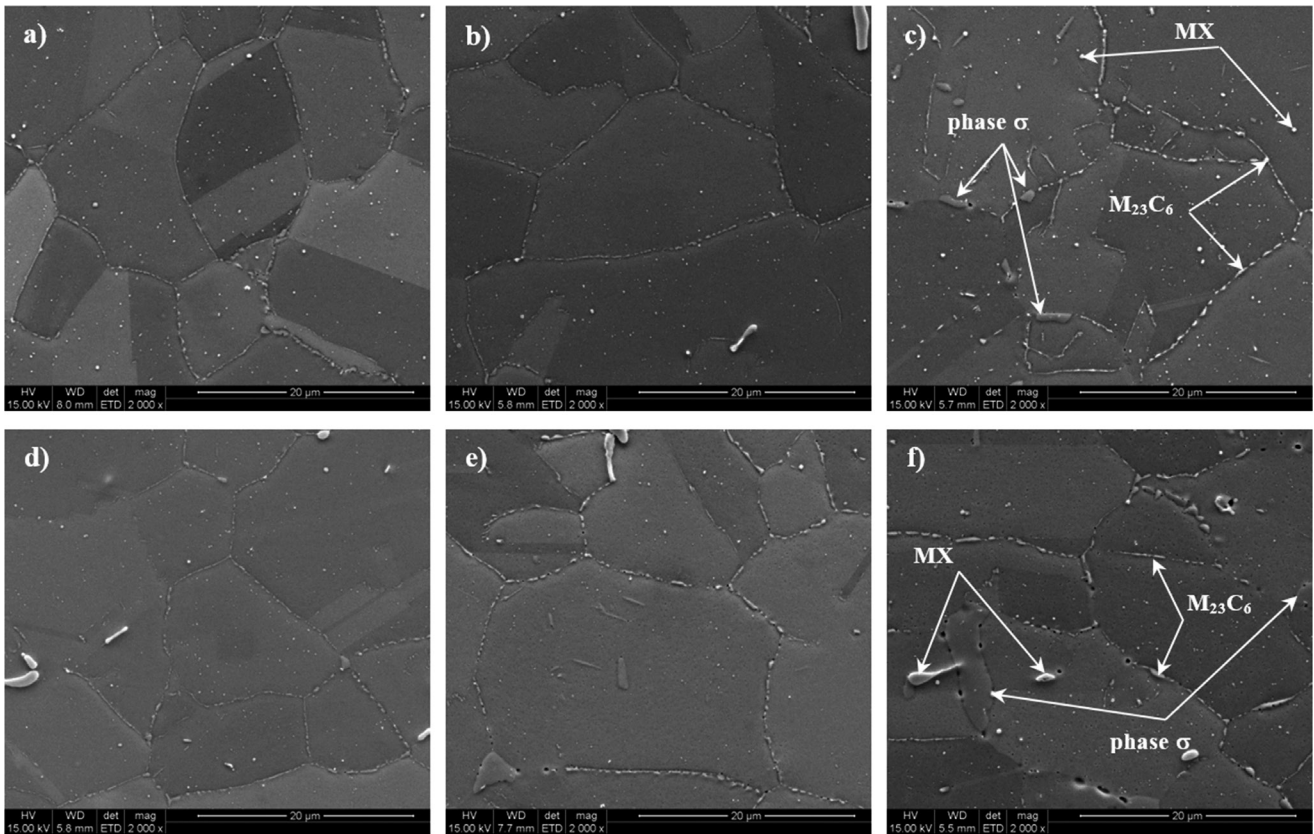


Fig. 2. Microstructure of S304H steel after ageing: at 650°C for a) 1 000 h, b) 10 000 h, c) 30 000 h; at 700°C for d) 1 000 h, e) 10 000 h, f) 30 000 h, SEM

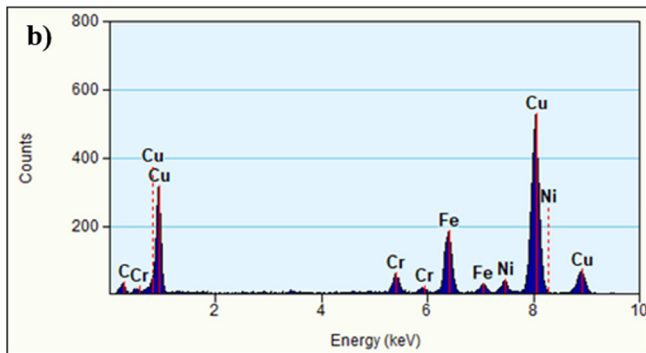
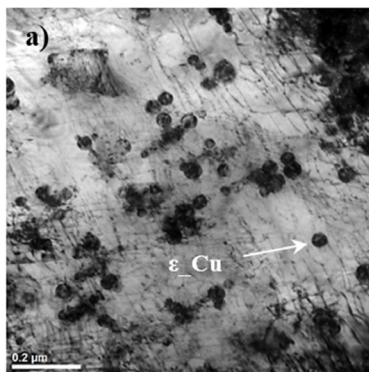


Fig. 3. a) Dislocation structure with ϵ -Cu phase precipitates after ageing at 650°C for 30 000 hours. Thin TEMBF film; b) EDX chemical composition of the precipitates from the area a) STEM

Using the results of metallographic tests, examples of which are shown in Figs 2 and 3, registering the precipitation processes occurring in the microstructure of S304H steel, both inside and along grain boundaries, their statistical analysis was carried out. Numerous publications indicate that the described precipitates significantly affect the properties of the tested material [9, 10, 21].

An example of the procedure for conducting image analysis in order to extract the precipitates of the analyzed phase is presented in Fig. 4. The percentage content of the phase in the total area of the analyzed image was calculated based on the surface area measurement. The average diameter equivalent to a given set was determined to unequivocally define the average particle size. The calculated statistical measures describing the empirical distributions of the equivalent diameter of the precipitates are presented in Tables 3–5.

Sample histograms of the distribution of the average equivalent diameter of the precipitate size and selected histograms describing the distribution of the surface area of the analyzed phases ($M_{23}C_6$, σ phase) for the most characteristic material states are presented in Figs 5, 6.

Depending on the chemical composition of the steel, $M_{23}C_6$ precipitates are generally characterized by low thermal stability during prolonged exposure to elevated temperatures. This leads to a relatively rapid increase in the average diameter of these precipitates and a decrease in their content in the microstruc-

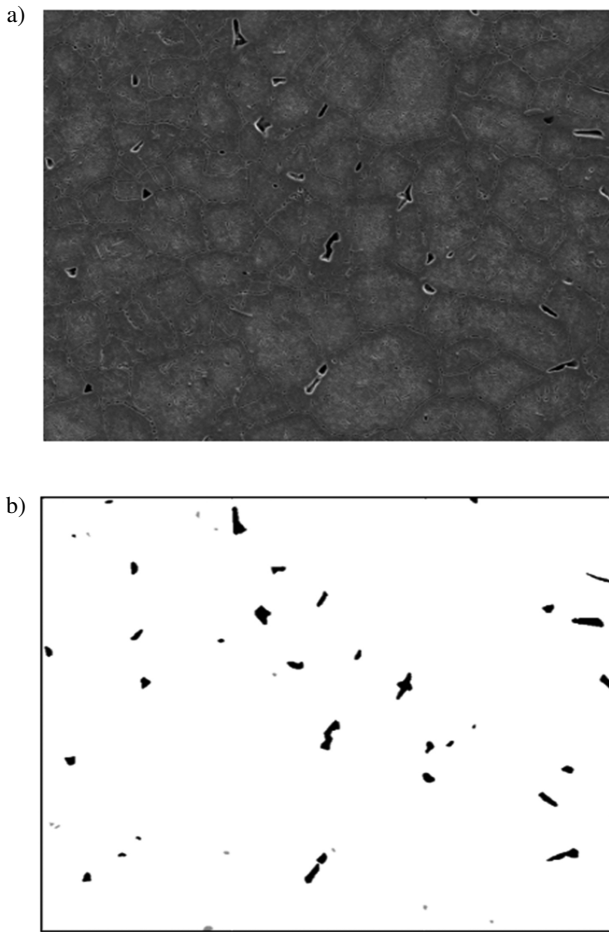


Fig. 4. Image analysis of σ phase precipitates of S304H steel after 10000 hours of ageing at 700°C; a) original image, b) binary image

Table 3

Statistical measures of the equivalent diameter of $M_{23}C_6$ precipitates in S304H steel

Testing material	Min. diameter μm	Max. diameter μm	Average diameter μm	Standard deviation	Surface fraction %
Ageing 1 000/650°C	0.08	0.97	0.30	0.2	2.01
Ageing 10 000/650°C	0.06	1.03	0.28	0.13	1.62
Ageing 30 000/650°C	0.06	1.07	0.34	0.14	1.65
Ageing 1 000/700°C	0.1	0.8	0.31	0.14	1.63
Ageing 10 000/700°C	0.06	1.0	0.33	0.14	1.65
Ageing 30 000/700°C	0.11	1.48	0.40	0.22	1.09

ture with the extension of the time of exposure to the ageing temperature. Under the adopted ageing conditions, the tested steel showed relative stability of the geometrical features of the

Table 4

Statistical measures of the equivalent diameter of the σ phase precipitates in S304H steel

Testing material	Min. diameter μm	Max. diameter μm	Average diameter μm	Standard deviation	Surface fraction %
Ageing 1 000/650°C	0	0	0	0	0
Ageing 10 000/650°C	0.76	2.47	1.39	0.44	0.39
Ageing 30 000/650°C	0.56	4.04	1.58	0.81	2.24
Ageing 1 000/700°C	0	0	0	0	0
Ageing 10 000/700°C	0.86	5.11	2.39	1.28	1.09
Ageing 30 000/700°C	0.65	8.40	2.12	1.53	4.44

Table 5

Statistical measures of the equivalent diameter of ϵ -Cu precipitates in S304H steel

Testing material	Min. diameter μm	Max. diameter μm	Average diameter μm	Standard deviation	Surface fraction %
Ageing 1 000/650°C	6.4	26.9	12.8	3.9	12.4
Ageing 10 000/650°C	11.2	84.7	33.8	20.0	27.2
Ageing 30 000/650°C	16.0	81.3	42.2	15.1	40.4
Ageing 1 000/700°C	9.0	65.7	22.7	12.6	19.7
Ageing 10 000/700°C	23.3	71.0	44.7	11.0	44.0
Ageing 30 000/700°C	40.5	129.0	71.3	21.2	71.1

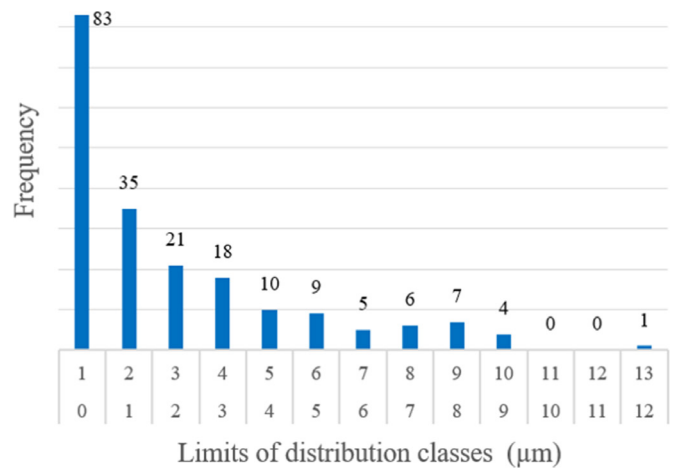


Fig. 5. Results of quantitative analysis of the surface area of σ phase after 30 000 hours of ageing at the temperature of 700°C

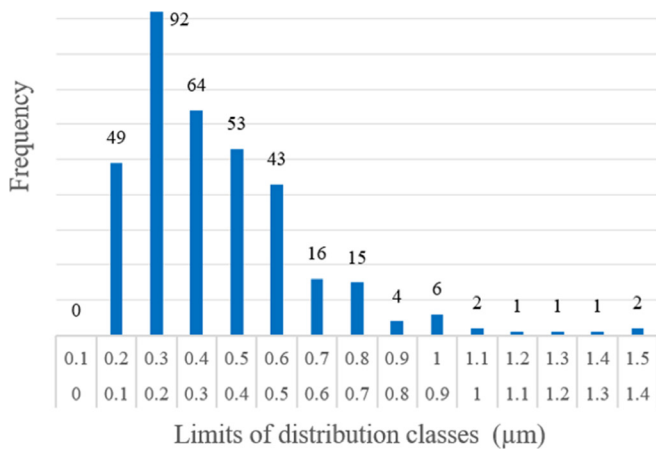


Fig. 6. Results of quantitative analysis of the surface area of $M_{23}C_6$ precipitates after 30 000 hours of ageing at the temperature of 700°C

particles, and a clear effect of changing the morphology of these precipitates was observed only after ageing for 30 000 hours at 700°C .

On the other hand, their quantitative share, measured by the surface area of a cross-section, decreases with increasing ageing time and temperature, which is the result of their disappearance due to the development of changes related to σ phase precipitation.

The results of the measurement of statistical average equivalent diameter of the σ phase precipitates show that the identifiable occurrence of the σ phase particles takes place after ageing for 10 000 hours with an average diameter of $1.39\ \mu\text{m}$. As the ageing time is extended up to 30 000 hours, the average particle size increases to $1.58\ \mu\text{m}$, i.e. by about 14%. On the other hand, the share of the σ phase, measured by the surface area of the planar particle cross-section, increases significantly with ageing time and temperature from the value of 0.39 after ageing at $650^\circ\text{C}/10\ 000$ hours to 4.44 after ageing $700^\circ\text{C}/30\ 000$ hours. The results of analogous measurement for the ageing temperature of 700°C indicate advancement of the precipitation process and increase in the average diameter of the σ phase particles to $2.39\ \mu\text{m}$ with the ageing time of 10 000 hours as compared to the temperature of 650°C , i.e. by about 70%. Extension of the ageing time up to 30 000 hours causes a slight reduction of the particles' average diameter, to $2.12\ \mu\text{m}$, which probably results from the σ phase precipitation mechanism and the participation of chromium carbides in this process.

Finely-dispersed $\epsilon\text{-Cu}$ precipitates inside the grains of the tested steel are characterized by quite high stability. The observation of the precipitates using TEM techniques (Fig. 7) indicates a continuous but slow increase in the particle size of the copper-rich phase along with the ageing time. This increase will ensure that the steel maintains high strength properties over a long period of operation (Table 5). These particles are

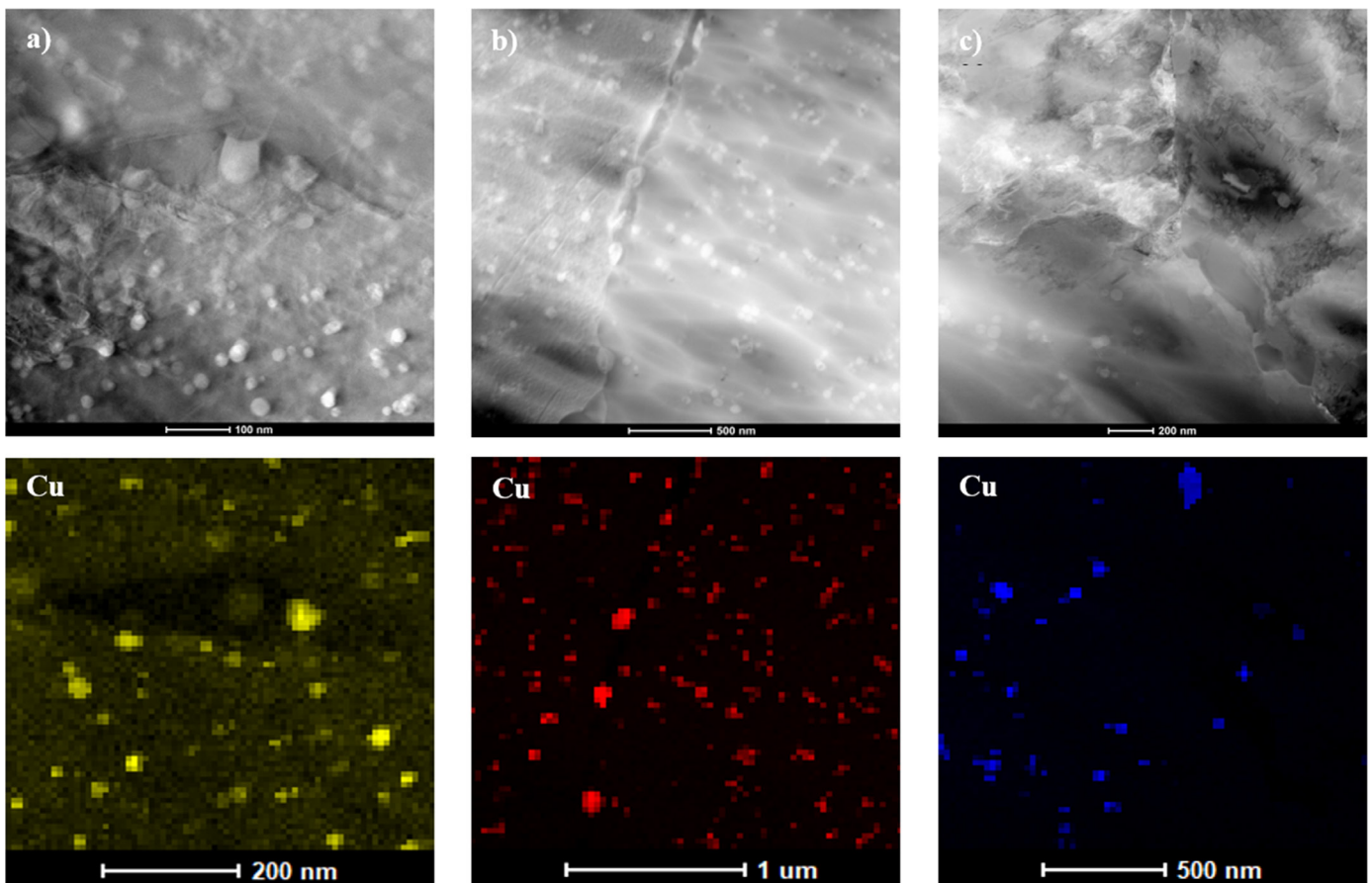


Fig. 7. $\epsilon\text{-Cu}$ precipitates in S304H steel after ageing at 700°C , a) 1 000 h, b) 10 000 h, c) 30 000 h

precipitated already in the first hour of ageing in the temperature range of 650–700°C. In [22], these types of precipitates with a size of approx. 2 nm were revealed after one hour of ageing at 650°C. According to the literature, in copper-rich precipitates in the initial period of ageing, the copper content is about 17%, with an additional content of elements such as: iron (approx. 55%), chromium (approx. 20%) and nickel (approx. 10%). Longer ageing time, i.e. about 500 hours at the temperature of 650°C, increased the copper content in the precipitate to approx. 90% [15]. The obtained results of the ϵ -Cu phase measurements indicate that with the increase of the ageing time and the temperature increase to 700°C, there is a continuous increase in the particle's average diameter, respectively for the temperature of 650°C from 12.8 nm to 42.2 nm and from 22.7 nm to 71.3 nm for a temperature of 700°C.

4. SUMMARY

As delivered, S304H steel is characterized by an austenitic microstructure with twins and numerous MX particles, locally arranged in bands, of various sizes inside and along grain boundary. When subjecting the tested material to long-term heat treatment, it was found that over time it was characterized by a very diverse microstructure. In the initial period of ageing, an intensive precipitation process takes place, during which numerous, very fine copper particles coherent with the matrix are released inside the grains. The second identified precipitate appearing in the structure of the tested steel are carbides, which are mainly released at grain boundaries. They were also observed inside the grains at longer ageing times. Long-term ageing also contributed to the precipitation of an unfavorable σ phase initially at boundaries, and after longer ageing also inside austenite grains. Its location and the tendency to significantly grow with ageing result in a significant reduction of functional properties. Its size and surface fraction can be used to assess the degree of degradation/loss of durability of components operating under creep conditions for a long time.

ACKNOWLEDGEMENTS

The results in this publication were obtained as part of research co-financed by the National Science Centre under contract 2011/01/D/ST8/07219 – Project: “Creep test application to model lifetime of materials for modern power generation industry” and co-financed with a rector's grant in the area of scientific research and development works, Silesian University of Technology, 10/010/RGJ21/1032.

REFERENCES

- [1] “Poland's Energy Policy PEP2040”, [Online]. Available: <https://www.gov.pl/web/klimat/polityka-energetyczna-polski>, [Accessed: 1. Mar. 2021].
- [2] M. Bartecka, P. Terlikowski, M. Klos, and Ł. Michalski, “Sizing of prosumer hybrid renewable energy systems in Poland,” *Bull. Pol. Acad. Sci. Tech. Sci.*, vol. 68, no. 4, pp. 721–731, 2020, doi: 10.24425/bpasts.2020.133125.
- [3] G. Golański, A. Zieliński, and A. Zielińska-Lipiec, “Degradation of microstructure and mechanical properties in martensitic cast steel after ageing,” *Materialwiss. Werkst.*, vol. 46, no. 3, pp. 248–255, 2015, doi: 10.1002/mawe.201400325.
- [4] J. Horváth, J. Janovec, and M. Junek, “The Changes in Mechanical Properties of Austenitic Creep Resistant Steels SUPER 304H and HR3C Caused by Medium-Term Isothermal Ageing,” *Sol. St. Phen.*, vol. 258, pp. 639–642, 2017, doi: 10.4028/www.scientific.net/ssp.258.639.
- [5] A. Zieliński, G. Golański, and M. Sroka, “Evolution of the microstructure and mechanical properties of HR3C austenitic stainless steel after ageing for up to 30,000 h at 650–750°C,” *Mat. Sci. Eng. A-Struct.*, vol. 796, p. 139944, 2020, doi: 10.1016/j.msea.2020.139944.
- [6] G. Golański, A. Zieliński, M. Sroka, and J. Słania, “The Effect of Service on Microstructure and Mechanical Properties of HR3C Heat-Resistant Austenitic Stainless Steel,” *Materials*, vol. 13, no. 6, p. 1297, 2020, doi: 10.3390/2Fma13061297.
- [7] A.F. Padilha and P.R. Rios, “Decomposition of Austenite in Austenitic Stainless Steels,” *ISIJ Intern.*, vol. 42, no. 4, pp. 325–327, 2002, doi: 10.2355/isijinternational.42.325.
- [8] R.L. Plaut, C. Herrera, D.M. Escriba, P.R. Rios, and A.F. Padilha, “A Short review on wrought austenitic stainless steels at high temperatures: processing, microstructure, properties and performance,” *Mater. Res.*, vol. 10, no. 4, pp. 453–460, 2007, doi: 10.1590/s1516-14392007000400021.
- [9] X. Xie, Y. Wu, C. Chi, and M. Zhang, “Superalloys for Advanced Ultra-Super-Critical Fossil Power Plant Application,” *Superalloys*, 2015, doi: 10.5772/61139.
- [10] A. Zieliński, G. Golański, M. Kierat, M. Sroka, A. Merda, and K. Sówka, “Microstructure of HR6W Alloy at Elevated Temperature after Prolonged Ageing in Air Atmosphere,” *Acta Phys. Pol. A*, vol. 138, no. 2, pp. 253–256, 2020, doi: 10.12693/aphyspola.138.253.
- [11] M. Sroka, A. Zieliński, A. Śliwa, M. Nabiałek, Z. Kania-Pifczyk, and I. Vasková, “The Effect of Long-Term Ageing on the Degradation of the Microstructure the Inconel 740h Alloy,” *Acta Phys. Pol. A*, vol. 137, no. 3, pp. 355–360, 2020, doi: 10.12693/aphyspola.137.355.
- [12] A. Zieliński, M. Sroka, and T. Dudziak, “Microstructure and Mechanical Properties of Inconel 740H after Long-Term Service,” *Materials*, vol. 11, no. 11, p. 2130, 2018, doi:10.3390/ma11112130.
- [13] A. Zieliński, J. Dobrzański, H. Purzyńska, R. Sikora, M. Dziuba-Kałuża, and Z. Kania, “Evaluation of Creep Strength of Heterogeneous Welded Joint in HR6W Alloy and Sanicro 25 Steel,” *Arch. Metall. Mater.* vol. 62, no. 4, pp. 2057–2064, 2017, doi: 10.1515/amm-2017-0305.
- [14] M. Sroka, A. Zieliński, A. Hernas, Z. Kania, R. Rozmus, T. Tański, and A. Śliwa, “The effect of long-term impact of elevated temperature on changes in the microstructure of inconel 740H alloy,” *Metallurgija*, vol. 56, no. 3–4, pp. 333–336, 2017.
- [15] M. Sroka, M. Nabiałek, M. Szota, and A. Zieliński, “The Influence of the Temperature and Ageing Time on the NiCr23Co12Mo Alloy Microstructure,” *Rev. Chim-Bucharest.*, vol. 68, no. 4, pp. 737–741, 2017, doi: 10.37358/rc.17.4.5541.
- [16] T. Tomaszewski, P. Strzelecki, M. Wachowski, and M. Stopel, “Fatigue life prediction for acid-resistant steel plate under operating loads,” *Bull. Pol. Acad. Sci. Tech. Sci.*, vol. 68, no. 4, pp. 913–921, doi: 10.24425/bpasts.2020.134184.

Analysis of the precipitation process of secondary phases after long-term ageing of S304H steel

- [17] A. Zieliński, M. Miczka, and M. Sroka, "The effect of temperature on the changes of precipitates in low-alloy steel," *Mater. Sci. Tech-Lond.*, vol. 32, no. 18, pp. 1899–1910, 2016, doi: [10.1080/02670836.2016.1150242](https://doi.org/10.1080/02670836.2016.1150242).
- [18] T. Tokairin *et al.*, "Investigation on long-term creep rupture properties and microstructure stability of Fe–Ni based alloy Ni–23Cr–7W at 700°C," *Mat. Sci. Eng. A-Struct.*, vol. 565, pp. 285–291, 2013, doi: [10.1016/j.msea.2012.12.019](https://doi.org/10.1016/j.msea.2012.12.019).
- [19] G. Golański, C. Kolan, A. Zieliński, and P. Urbańczyk, Degradation process of heat-resistant austenitic stainless steel, *Energetics*, vol. 11, pp. 727–730, 2017 [in polish].
- [20] M. Igarashi, Alloy design philosophy of creep – resistant steels In: Abe F., Kern T.U., Viswanathan R. (ED.), Creep resistant steels. Cambridge: Woodhead Publishing, 2008.
- [21] C. Chi, H. Yu, J. Dong, W. Liu, S. Cheng, Z. Liu, and X. Xie, "The precipitation strengthening behavior of Cu-rich phase in Nb contained advanced Fe–Cr–Ni type austenitic heat resistant steel for USC power plant application," *Prog. Nat. Sci.*, vol. 22, no. 3, pp. 175–185, 2012., doi: [10.1016/j.pnsc.2012.05.002](https://doi.org/10.1016/j.pnsc.2012.05.002).
- [22] H. Yu and Ch. Chi, "Precipitation behaviour of Cu-rich phase in 18Cr9Ni3CuNbN austenitic heat – resistant steel at early aging state", *Chin. J. Mater. Res.*, vol. 29, pp. 195–200, 2015.